ONCOIMMUNOLOGY
2022, VOL. 11, NO. 1, e2096572 (16 pages)
https://doi.org/10.1080/2162402X.2022.2096572

Taylor & Francis
Taylor & Francis Group

ORIGINAL RESEARCH

OPEN ACCESS Check for updates

Local delivery of interleukin 7 with an oncolytic adenovirus activates tumor-infiltrating lymphocytes and causes tumor regression

Tatiana V. Kudling[a], James H.A. Clubb[a,b], Dafne C.A. Quixabeira[a], Joao M. Santos[a,b], Riikka Havunen[a,b], Alexander Kononov[c], Camilla Heiniö[a], Victor Cervera-Carrascon[a,b], Santeri Pakola[a,d], Saru Basnet[a], Susanna Grönberg-Vähä-Koskela[a,d], Victor Arias[a], Ivan Gladwyn-Ng[e], Katri Aro[d,f], Leif Bäck[d,f], Jari Räsänen[g], Ilkka Ilonen[g], Kristian Borenius[g], Mikko Räsänen[g], Otto Hemminki[d,h], Antti Rannikko[d,h], Anna Kanerva[a,d,i], Johanna Tapper[d,i], and Akseli Hemminki [a,b,d]

[a]Cancer Gene Therapy Group, Translational Immunology Research Program, Faculty of Medicine, University of Helsinki, Helsinki, Finland; [b]TILT Biotherapeutics Ltd, Helsinki, Finland; [c]Systems Oncology Group, Cancer research UK, Manchester University, Manchester, UK; [d]Comprehensive Cancer Center, Helsinki University Hospital (HUS), Helsinki, Finland; [e]Taconic Biosciences GmbH, Leverkusen, Germany; [f]Department of Otorhinolaryngology – Head and Neck Surgery, Helsinki Head and Neck Center, Helsinki University Hospital and University of Helsinki, Helsinki, Finland; [g]Department of Thoracic Surgery, Heart and Lung Center, Helsinki University Hospital and Faculty of Medicine, University of Helsinki, Helsinki, Finland; [h]Department of Urology, Helsinki University Hospital, Helsinki, Finland; [i]Department of Gynecology and Obstetrics, Helsinki University Hospital, Helsinki, Finland

ABSTRACT

Cytokines have proven to be effective for cancer therapy, however whilst low-dose monotherapy with cytokines provides limited therapeutic benefit, high-dose treatment can lead to a number of adverse events. Interleukin 7 has shown promising results in clinical trials, but anti-cancer effect was limited, in part due to a low concentration of the cytokine within the tumor. We hypothesized that arming an oncolytic adenovirus with Interleukin 7, enabling high expression localized to the tumor microenvironment, would overcome systemic delivery issues and improve therapeutic efficacy. We evaluated the effects of Ad5/3-E2F-d24-hIL7 (TILT-517) on tumor growth, immune cell activation and cytokine profiles in the tumor microenvironment using three clinically relevant animal models and *ex vivo* tumor cultures. Our data showed that local treatment of tumor bearing animals with Ad5/3- E2F-d24-hIL7 significantly decreased cancer growth and increased frequency of tumor-infiltrating cells. Ad5/3-E2F-d24-hIL7 promoted notable upregulation of pro-inflammatory cytokines, and concomitant activation and migration of CD4+ and CD8 + T cells. Interleukin 7 expression within the tumor was positively correlated with increased number of cytotoxic CD4+ cells and IFNg-producing CD4+ and CD8+ cells. These findings offer an approach to overcome the current limitations of conventional IL7 therapy and could therefore be translated to the clinic.

ARTICLE HISTORY
Received 23 February 2022
Revised 9 June 2022
Accepted 24 June 2022

KEYWORDS
Oncolytic virus; adenovirus; interleukin 7; immunotherapy

Introduction

Cytokines are small protein molecules that provide growth, differentiation, and inflammatory or anti-inflammatory signals to different cell types. Cytokine immunotherapy is an appealing approach for treating cancer patients with advanced malignancies because signals transduced via cytokines activate the host immune system, making it more efficient in the recognition and elimination of cancer cells. However, to date, only two cytokines – interleukin 2 (IL2) and interferon-alpha – are approved by the U.S. Food and Drug Administration for cancer treatment.[1,2] Both of them can stimulate the proliferation and activation of T cells, but high concentrations are needed to achieve therapeutic efficacy in cancer patients. Consequently, increasing the systemic dose results in adverse events before sufficient tumor concentrations can be reached.[3–5]

Interleukin 7 (IL7) is one of the key cytokines involved in immune cell expansion and proliferation. Its main function is to maintain the survival and diversity of naïve and memory T cells.[6,7] IL7 can improve the effector functions of T cells via repression of negative regulators of T cell activation and increase interferon gamma (IFNg) production.[8] Conversely, IL7 antagonizes the immunosuppressive pathways via several mechanisms. It prevents the activation of regulatory T cells (Tregs) and inhibits their ability to suppress effector cells.[9] Further, IL7 abrogates inhibition of CD8 + T cell proliferation and prevents their exhaustion.[10,11]

Possessing multiple immune-enhancing features, IL7 is an attractive cytokine for immunotherapy. In contrast to IL2 and interferon-alpha, it showed a reasonable safety profile in phase I clinical trials, even at the highest studied dose.[12] Moreover, IL7 treatment leads to a remarkable increase in circulating CD4 + and CD8 + T cells, both naïve and memory; however, no effect on tumor progression and overall survival of cancer patients was observed in these studies.[13] One possible reason is the inability to reach sufficient concentrations of IL7 within the tumor with systemic delivery. Thus, recent studies describe new approaches for IL7 delivery, including IL7 fusion proteins

CONTACT Akseli Hemminki akseli.hemminki@helsinki.fi Cancer Gene Therapy Group, Translational Immunology Research Program, Faculty of Medicine, University of Helsinki, Helsinki, Finland
Supplemental data for this article can be accessed online at https://doi.org/10.1080/2162402X.2022.2096572

able to circulate longer *in vivo*,[14] and engineered immune cells constitutively expressing IL7.[15,16] However, these technologies are still in the developmental stage, so it remains unclear if they will be safe and effective in the clinic.

In this study, we developed an oncolytic adenovirus coding for the full length human IL7 sequence – Ad5/3-E2F-d24-hIL7 (TILT-517). It combines the capability to maintain high concentrations of IL7 in the tumor microenvironment with the inherent ability of adenovirus to stimulate an immune response. Together this can lead to increased immune cell infiltration to the tumor and activation of antiviral signaling pathways, converting the local microenvironment from an immunosuppressive to an immunostimulatory one. Moreover, since Ad5/3-E2F-d24-hIL7 is modified to replicate specifically in malignant cells, this approach enables effective oncolysis of cancer cells and reduced probability of adverse off-target effects of the treatment.

In the last two years, there has been increased efforts to develop oncolytic viruses armed with IL7. One study highlighted the antitumor activity of an oncolytic vaccinia virus encoding IL7 and IL12 in both injected and non-injected tumors, through immune status changes in humanized mice bearing human cancer cells.[17] Another study described the benefits of using IL7 loaded oncolytic adenovirus in combination with CAR-T in glioblastoma, enabling survival and therapeutic efficacy of the cells.[18] However, chimeric oncolytic adenoviruses armed with IL7 as a monotherapy have not been studied. In this paper, we describe lytic and immune-enhancing features of the virus in several preclinical models shedding the light on its potential for translation to the clinic.

Methods

Cell lines

Human cancer cell lines A549 (lung adenocarcinoma) and RD (rhabdomyosarcoma) were purchased from the American Type Culture Collection (ATCC) (Manassas, USA). The Syrian hamster cancer cell line DDT1-MF2 (leiomyosarcoma) was a kind gift from Dr. William Wold, hamster HapT1 (pancreatic ductal adenocarcinoma) was obtained from Leibniz Institute (DSMZ, Braunschweig, Germany), hamster HT100 (lung adenocarcinoma) was obtained from the Japanese Collection of Research Bioresources Cell Bank (Osaka, Japan). All cell lines were cultured under recommended conditions.

Virus construction

The Ad5/3-E2F-d24-hIL7 virus has been constructed by a previously described technique.[19] Tumor-specific replication was achieved by two modifications: an E2F promoter and a 24-base pair deletion in the constant region of E1A, which determines tumor selectivity regarding viral replication. Human IL7 (hIL7) coding sequence (Genbank: NP_000871.1) was introduced in E3 region replacing gp19k and 6.7k genes via bacterial artificial chromosome (BAC) recombineering strategy.[20] The resulting viral vector sequence was confirmed by next generation sequencing.

Viral particles were produced via cesium chloride gradient centrifugation, and the infectivity and concentration of the resulting virus were determined by TCID50 assay according to a protocol described elsewhere.[21]

Cell viability assay

Human cell lines A549 and RD were plated in 96-well plates (flat bottom) in triplicates at 1×10^4 cells/well for 24 hours and infected with 1, 10, 100 or 1000 VP/cell of either Ad5/3-E2F-d24 virus (also referred in the text as backbone or unarmed backbone), or Ad5/3-E2F-d24-hIL7 (also referred in the text as IL7 virus). Similarly, hamster cell lines HT100, DDT1-MF2 and HapT1 were plated in triplicates at 1×10^4 cells/well for 24 hours and infected with 100, 1000, 5000 or 10000 VP/cell of either backbone virus, or Ad5/3-E2F-d24-hIL7.

Cell viability was measured after 4 days (A549 and RD), 5 days (HT100 and DDT1-MF2) or 8 days (HapT1) by incubating cells for 2 hours with 20% of CellTiter 96 AQueous One Solution Proliferation Assay reagent (Promega, Wisconsin, USA). Absorbance was read at 490 nm using Hidex Sense plate reader (Hidex, Turku, Finland). Data were normalized to the uninfected mock control group.

Cytokine expression and bioactivity assay

The aforementioned human and hamster cell lines were infected with either 1000 VP/cell (A549 and RD) or 10000 VP/cell (HT100 and DDT1-MF2) of Ad5/3-E2F-d24-hIL7 for 3 days. Human IL7 concentration was measured from cell culture supernatants using the BD Cytometric Bead Array Human Soluble Protein Master Buffer Kit (BD Biosciences, New Jersey, USA) together with human IL7 Flex Set (BD Biosciences, New Jersey, USA) according to the manufacturer's instructions. The beads were detected with the BD Accuri Flow Cytometer and the results were analyzed with FCAP Array software (version 3.0.1; BD Biosciences, New Jersey, USA).

To confirm that virally produced hIL7 was bioactive, murine IL7-dependent cell line 2E8 (ATCC, Virginia, USA) was cultured in triplicates at 2.5×10^5 cells/ml in McCoy's 5A media (ThermoFisher, Massachusetts, USA) supplemented with 10% FBS, 1% L-glutamine and 1% Pen/strep for 24 hours. Supernatant from A549 cells infected with Ad5/3-E2F-d24-hIL7 was filtered to remove infectious virus particles and was added at 1:1, 1:4, 1:16, 1:64 and 1:256 dilutions and incubated for 5 days prior to viability assay using 20% of CellTiter 96 AQueous One Solution Proliferation Assay reagent as described above. Recombinant murine and human IL7 were used at 20 ng/ml concentration as positive controls.

IL7 cross-reactivity assay

Hamster splenocytes were seeded in 96-well plates (U-bottom) in triplicates at 2.5×10^5 cells/well for 24 hours to investigate if hamster immune cells cross-react to human IL7. Then the cells were stimulated with either Concanavalin A (ConA), or ConA in combination with recombinant hIL7 (Peprotech, New Jersey, USA) for 5 days. Unstimulated cells were used as

a negative control, while cells stimulated with ConA and recombinant hIL2 (Peprotech, New Jersey, USA) were used as a positive control. On day 5, the viability test was performed using 20% of CellTiter 96 AQueous One Solution Proliferation Assay reagent as described above.

Syngeneic hamster experimental model

HapT1 tumors ($2x10^6$ cells) were engrafted subcutaneously in 5 weeks old male Syrian golden hamsters' (*Mesocricetus auratus*) (Envigo, Indiana, USA) right flank. After tumors reached 5 to 6 mm in diameter, animals were randomized and treated intratumorally with 1×10^9 VP of either Ad5/3-E2F-d24 or Ad5/3-E2F-d24-hIL7 virus. Control animals received intratumoral injections of PBS. Tumors were measured every other day for 14 days with a digital caliper, and tumor volumes were calculated as (length x width^2)/2. Hamsters received a total of five rounds of virus treatment before they were euthanized on day 15, and their tumors were collected for subsequent analysis.

To study the toxicity of the virus, the aforementioned experiment was repeated, but animals were treated for 55 days with subsequent collection of lungs, hearts, livers, kidneys, and spleens for histopathological evaluation.

Gene expression assay

Fragments of animal tumor samples were preserved in RNAlater (Sigma-Aldrich, Missouri, USA), and stored at −20°C until further use. RNA from the samples were isolated using RNeasy extraction kit (Qiagen, Hilden, Germany) according to the manufacturer's instructions and RNA concentration was measured using Qubit4 Fluorometer (ThermoFisher, Massachusetts, USA). 250 ng of purified total RNA was used to synthetize cDNA with High capacity cDNA Reverse Transcription kit (ThermoFisher, Massachusetts, USA) according to the manufacturer's instructions. Resulting cDNA was used for quantitative real-time PCR. The expression levels of Granzyme B, Perforin, CD25, CD137, IFNg, and PD1 were measured using the primers and probes listed in Supplementary table S1. The results were normalized against the content of hamster gamma actin housekeeping gene cDNA and against mock (ΔΔCt method). All PCR reactions were run in duplicates.

Histopathology analysis

Selected tissues (livers, lungs, hearts, spleens and kidneys) collected for histopathological analysis were fixed in 10% formalin, and routinely processed and paraffin embedded. Samples paraffin-blocks were sectioned into 5 mm thickness slides and further stained with hematoxylin and eosin. A veterinarian pathologist examined the samples slides in a blind manner.

Patient samples processing and establishment of *ex vivo* tumor histocultures

Fresh single-cell tumor digests were prepared from tumors using a protocol previously developed by our group.[22] In brief, tumors were diced into small fragments and placed in a 50 mL falcon tube containing RPMI 1640 supplemented with 1% L-glutamine, 1% Pen/strep, collagenase type I (170 mg/L), collagenase type IV (170 mg/L), DNase I (25 mg/mL) and elastase (25 mg/mL) (all enzymes from Worthington Biochemical) for overnight enzymatic digestion with rocking at +37°C. After digestion, the cell suspension was filtered through a 70 μm filter and treated with ACK lysis buffer (Sigma-Aldrich, Missouri, USA) for the removal of undigested fragments and red blood cells. The resulting heterogeneous single-cell suspension was used to establish *ex vivo* tumor cultures by plating 3×10^5 viable cells in triplicates in a 96-well plate (U-bottom) and treating them with 100 VP/cell of either Ad5/3-E2F-d24 or Ad5/3-E2F-d24-hIL7 virus; uninfected cells were used as mock control. The cells were collected on day 3 in freezing media containing 90% fetal bovine serum (FBS) and 10% dimethyl sulfoxide and stored up to −140°C until further use for flow cytometry.

Cytotoxicity and virus replication assay

Cell viability of *ex vivo* tumor cultures was determined as described above. Briefly, cell viability was measured at days 3, 5 and 7 by incubating with 20% CellTiter 96 AQueous One Solution Proliferation Assay reagent for 2 hours. Data were normalized to uninfected control group.

In order to determine virus replication in *ex vivo* tumor cultures, the cells were collected in phosphate buffered saline on days 1, 2 and 3 after virus infection and the DNA was extracted with QIAmp DNA Mini Kit (Qiagen, Hilden, Germany) according to the manufacturer's instructions. Virus presence was confirmed by quantitative real-time PCR targeting the E4 region using forward primer (5′-GGAGTGCG CCGAGACAAC-3′), reverse primer (5′-ACTACGTC CGGCGTTCCAT-3′) and probe (Fam-TGGCATGACACTA CGACCAACACGATCT-Tam). Quantification of E4 was calculated according to a standard curve generated using known concentrations of a viral DNA. The results were normalized to the content of human beta-actin housekeeping gene. All PCR reactions were run in duplicates.

Chemokines and cytokines analysis

Supernatants from the infected *ex vivo* tumor cultures were collected on day 3 and the presence of C-C motif ligand 2 (Ccl2), C-C motif ligand 5 (Ccl5), C-X-C motif chemokine 10 (Cxcl10), interleukin 2 (IL2), tumor necrosis factor alpha (TNFa), IFNg, interferon 1 beta (IFN1b), interleukin 4 (IL4), interleukin 6 (IL6), interleukin 10 (IL10) and transforming growth factor beta (TGFb) was determined using the Essential Immune Response LEGENDplex panel (Biolegend, California, USA), according to the manufacturer's instructions.

The levels of C-X-C motif chemokine 9 (Cxcl9; also known as MIG) and IL7 in supernatants were determined through human MIG and IL7 flex sets (BD Biosciences, New Jersey, USA) respectively. Samples were measured in triplicates using Accuri C6 flow cytometer and analyzed through either LEGENDplex Data Analysis Software Suite (Biolegend, California, USA) or FCAP Array software. The concentration of each analyte was

normalized to the total protein content measured via Qubit4 Fluorometer (ThermoFisher, Massachusetts, USA). This data was then normalized to uninfected control group.

Migration assay

Ex vivo tumor single cell suspensions were cultured at 3×10^5 viable cells in triplicates in a 96-well plate (U-bottom) using serum-free AIM-V media (ThermoFisher, Massachusetts, USA) and treated with either Ad5/3-E2F-d24 or Ad5/3-E2F-d24-hIL7 as described above. On day 3, supernatants were collected and plated in the bottom chamber of Transwell (Corning, New York, USA) with a 5 µM pore membrane. 5×10^5 PBMCs were added in the upper chamber and left for migration for 24 h.

After migration, the cells in the bottom chamber were stained with following antibodies: PE anti-human CD45, Alexa Fluor 700 anti-human CD3, V500 anti-human CD4, FITC anti-human CD8, PerCP-Cy5.5 anti-human CD56, APC anti-human CD14, APC-Cy7 anti-human CD11b, BV421 anti-human CD83 and PE-Texas Red anti-human CD206 (Supplementary table S2). Absolute cell count was performed using 123count eBeads (Invitrogen, Massachusetts, USA) according to the manufacturer's recommendations. Samples were acquired in triplicates using FACS Aria II cell sorter (BD Biosciences, New Jersey, USA) collecting at least 50000 events per sample. Data analysis was performed using Flowjo software v10 (Flowjo LLC, BD Biosciences, New Jersey, USA).

Cell sorting and RNA sequencing

CD4+ and CD8 + T cells from *ex vivo* tumor cultures were labeled using following antibodies: FITC anti-human CD3 antibody (clone SK7, Biolegend, California, USA), PE anti-human CD8 antibody (clone SK1, Biolegend, California, USA) and PerCP-Cyanine5.5 anti-human CD4 antibody (clone RPA-T4, ThermoFisher, Massachusetts, USA). Sorting was performed on Sony SH800z sorter (SONY) using 100-µm microfluidic sorting chip with at least 90% purity.

RNA from the sorted cells was isolated using RNAqueous Micro Total RNA Isolation Kit (ThermoFisher, Massachusetts, USA) according to the manufacturer's instructions, and measured with Qubit4 Fluorometer. Sequencing was performed by GENEWIZ (Germany) using PolyA selection and 20–30 million reads per sample. Comparison of gene expression between groups was performed using DESeq2, the Wald test was used to generate p-values and log2 fold changes. Genes with an adjusted p-value < 0.05 were called as differentially expressed genes.

Human PBMC isolation and expansion

Human PBMC isolation was performed through density gradient centrifugation with lymphoprep (StemCell technologies, Vancouver, Canada) according to the manufacturer's recommendations.

PBMC expansion was carried out according to adjusted "rapid expansion" protocol published elsewhere.[23] Briefly, 1×10^7 cells were placed into six-well G-rex culturing plates (Wilson Wolf, Minnesota, USA) filled with 30 mL of TIL medium (TM) containing RPMI 1640 supplemented with 20% FBS, 1% L-glutamine, 1% Pen/strep, 15 mM HEPES, 1 mM Na-pyruvate, 50 µM b-mercaptoethanol, 100 IU/mL recombinant human IL-2 (PeproTech, New Jersey, USA) and 50 ng/ml anti-human anti-CD3 antibody (clone OKT3, Invitrogen, Massachusetts, USA). Subsequently, the cells were incubated for 3 days in a humidified incubator at +37°C. At day 3, PBMCs were mixed with irradiated allogenic PBMCs at 1:200 ratio in 1:1 media (50% TM, 50% Rapid Expansion Media (REM), containing RPMI 1640 supplemented with 20% FBS, 1% L-glutamine, 1% Pen/strep and 100IU/mL recombinant human IL-2) and seeded to G-rex culturing plates at 2×10^6 cells/well. After 5 days of incubation half of the media was replaced with fresh 1:1 TM and REM media. By day 7, half of the media was aspirated (while retaining the cells in the bottom) and the number of PBMCs was adjusted to 5×10^6 cells/well every 3–4 days until day 14, in which PBMCs were collected in freezing medium and stored up to −140°C until further use.

Generation of murine PDX ovarian cancer model (PDX-OvCa)

A metastasis resected from the greater omentum of a patient bearing ovarian high-grade serous carcinoma stage IIIC was collected, digested and frozen, in accordance with previously described protocols.[22] For the generation of a patient-derived xenograft (PDX), cells were thawed, resuspended in a 1:1 Matrigel/RPMI medium containing 1% P/S and 1% L-Glut and implanted in the lower lateral flanks of NOG mice (strain *NOD.Cg-Prkdc^{scid}Il2rg^{tm1Sug}/JicTac*, Taconic Biosciences GmbH, Leverkusen, Germany) (n = 3 with 2 tumors per mice). Animals were followed regularly for the development of tumors. Approximately, 6 months after the first engraftment, developed tumors were collected, processed as above and reinjected into new NOG mice. In the second engraftment, tumors were harvested approximately 4 months later. Tumor samples were processed and cultured in vitro using 10% RPMI growth media until they started to grow normally. Cell were stored in freezing media at −80 C.

PDX-OvCa murine experimental models (NOG and NOG-IL2)

3 to 4 weeks old immunodeficient female NOG (strain *NOD.Cg-Prkdc^{scid}Il2rg^{tm1Sug}/JicTac*) and NOG-IL2 (*strain NOD.Cg-Prkdc^{scid}Il2rg^{tm1Sug} Tg(CMV-IL2)4–2Jic/JicTac*) mice were obtained from Taconic Biosciences GmbH, Leverkusen, Germany. Animals were engrafted subcutaneously in the lower lateral flank with 3.5×10^6 PDX-OvCa cell line in 50% Matrigel (Corning, New York, USA). After tumors reached 4 to 5 mm in diameter, animals received 3×10^6 autologous PBMCs infusion intraperitoneally. Next day they were randomized and treated intratumorally with 1×10^9 VP of either Ad5/3-E2F-d24 or Ad5/3-E2F-d24-hIL7 virus. Control animals received intratumoral injections of PBS. Tumors were measured with a digital caliper, and tumor volumes were calculated as (length

x width^2)/2. Mice received a total of six rounds of virus treatment before they were euthanized on day 16, and their tumors and blood were harvested for subsequent analysis.

Flow cytometry

Analysis of immune cells from hamster's tumor single-cell suspensions was performed using the following cross-reactive antibodies: PE-Cyanine7 anti-mouse CD4, PE anti-rat CD8b, Alexa Fluor 488 polyclonal anti-asialo-GM1, FITC anti-mouse /rat MHC class II (I-Ek) (Supplementary table S2).

Analysis of immune cell populations from *ex vivo* tumor cultures was performed using the following antibodies: V500 anti-human CD4, FITC anti-human CD8, PE-Cy7 anti-human CD69, PE-CF594 anti-human CD127, BV421 anti-human Granzyme B, PerCP-Cyanine5.5 anti-human Perforine, APC-Cyanine7 anti-human CD107a antibodies (Supplementary table S2). Intracellular staining was performed using BD Cytofix/Cytoperm Plus Kit (with BD GolgiPlug) (BD Biosciences, New Jersey, USA), according to manufacturer's instructions. Samples were stained after Fc blocking using Human TruStain FcX Receptor Blocking Solution (Biolegend, California, USA).

Analysis of immune cells from murine PDX-OvCa tumors was performed using the following antibodies: Alexa Fluor 700 anti-human CD3, V500 anti-human CD4, FITC anti-human CD8, PE-Cy7 anti-human CD69 (Supplementary table S2).

All samples were acquired in duplicates using FACS Aria II cell sorter (BD Biosciences, New Jersey, USA) collecting at least 50000 events per sample. Data analysis was performed using Flowjo software v10 (Flowjo LLC, BD Biosciences, New Jersey, USA).

Statistical analysis

GraphPad Prism v.8.4.2 (GraphPad Software) was used for statistical analysis and graphical representation of the data. The normality of tumor progression data was assessed using Shapiro–Wilk test, and the equality of variances – using Levene's test. To compare groups in animal experiments, two-way ANOVA with Tukey multiple comparisons test was used. Unpaired t-test was used to compare treated groups, and correlations between variables were investigated using Pearson correlation. Heatmaps for RNAseq data were designed using RStudio.

Results

An oncolytic adenovirus armed with human IL7 is able to deliver the transgene to cancer cells and lyse multiple cancer cell lines

Previously, we demonstrated the ability of Ad5/3-E2F-d24 viruses to penetrate and replicate in several cancer cell lines.[19] The oncolytic adenovirus coding for human IL7 utilizes the same backbone from adenovirus serotype 5 that carries the fiber knob from serotype 3, has a 24-bp deletion (d24) in the constant region 2 of the E1A gene and the insertion of a tumor-specific E2F promoter upstream the E1A region. Moreover, E1B 19 K gene was deleted to enhance the cytotoxicity of adenovirus by inducing early cell lysis and enhancing progeny release.[24] The human IL7 gene was introduced in the partially deleted E3 gene region, making the transgene expression linked to virus replication (Figure 1a).

The ability of Ad5/3-E2F-d24-hIL7 to infect and lyse cancer cells was evaluated *in vitro* using several human and hamster cell lines. Human lung and rhabdomyosarcoma cancer cell lines (A549 and RD, respectively), and hamster leiomyosarcoma, lung and pancreatic cancer cell lines (DDT1-MF2, HT100 and HapT1, respectively) were infected with different concentrations of Ad5/3-E2F-d24-hIL7; uninfected cells and cells infected with previously described[18] unarmed Ad5/3-E2F-d24 virus were used as controls. Accordingly, the lytic efficacy of Ad5/3-E2F-d24-hIL7 virus was comparable to the unarmed virus (Figures 1B and 1c). These results demonstrate that the presence of the IL7 transgene does not affect virus oncolytic features.

To assess the ability of the virus to induce transgene expression in cancer cells, A549 cell line was infected with Ad5/3-E2F-d24-hIL7 and culture supernatants were analyzed for the presence of IL7 protein levels. Notably, human cell lines showed higher concentration of IL7 with the maximum amount of 17.5 ng/ml produced by A549 (Figure 1d). Hamster cell line HT100 had the lowest protein level (0.4 ng/ml), while DDT1-MF2 and RD cell lines had similar productivity of around 2.5 ng/ml of IL7 (Figure 1d).

Next, we evaluated the bioactivity of human IL7 produced by the virus. To do this, we incubated IL7-dependent murine cell line 2E8 with several dilutions of A549 supernatant with subsequent cell proliferation measurement. We observed dose-dependent cell proliferation with the better outcome at 1:4 dilution compared to control group (Figure 1e).

To evaluate the suitability of the Syrian hamster animal model for analysis of Ad5/3-E2F-d24-hIL7 *in vivo* antitumor activity, we first assessed the cross-reactivity of human IL7 in Syrian hamsters. To do this, we stimulated hamster splenocytes with ConA and recombinant human IL7 and observed significantly increased proliferation rate compared to unstimulated cells and ConA alone ($p < .0001$ and $p = .0061$, respectively), while no significant difference was observed between the groups treated with IL7 and IL2 ($p = .6308$) (figure 1f).

Overall, we confirmed that Ad5/3-E2F-d24-hIL7 is capable of killing cancer cells and inducing the expression of bioactive IL7. Moreover, human IL7 is cross-reactive and can be used for *in vitro* and *in vivo* studies in Syrian hamsters.

IL7 oncolytic adenovirus promotes tumor regression in a hamster model of pancreatic cancer

The *in vivo* efficacy of Ad5/3-E2F-d24-hIL7 was tested in the immunocompetent Syrian hamster, a preclinical model semi-permissive to adenovirus replication. Pancreatic cancer cell line HapT1 was engrafted subcutaneously to allow heterotopic tumor formation and subsequent intratumoral virus injections (Figure 1g). 15 days after treatment initiation, hamsters in the mock control group had significantly larger tumors when compared to virus-treated animals. Both backbone and IL7 coding virus-treated groups showed a trend for the reduction

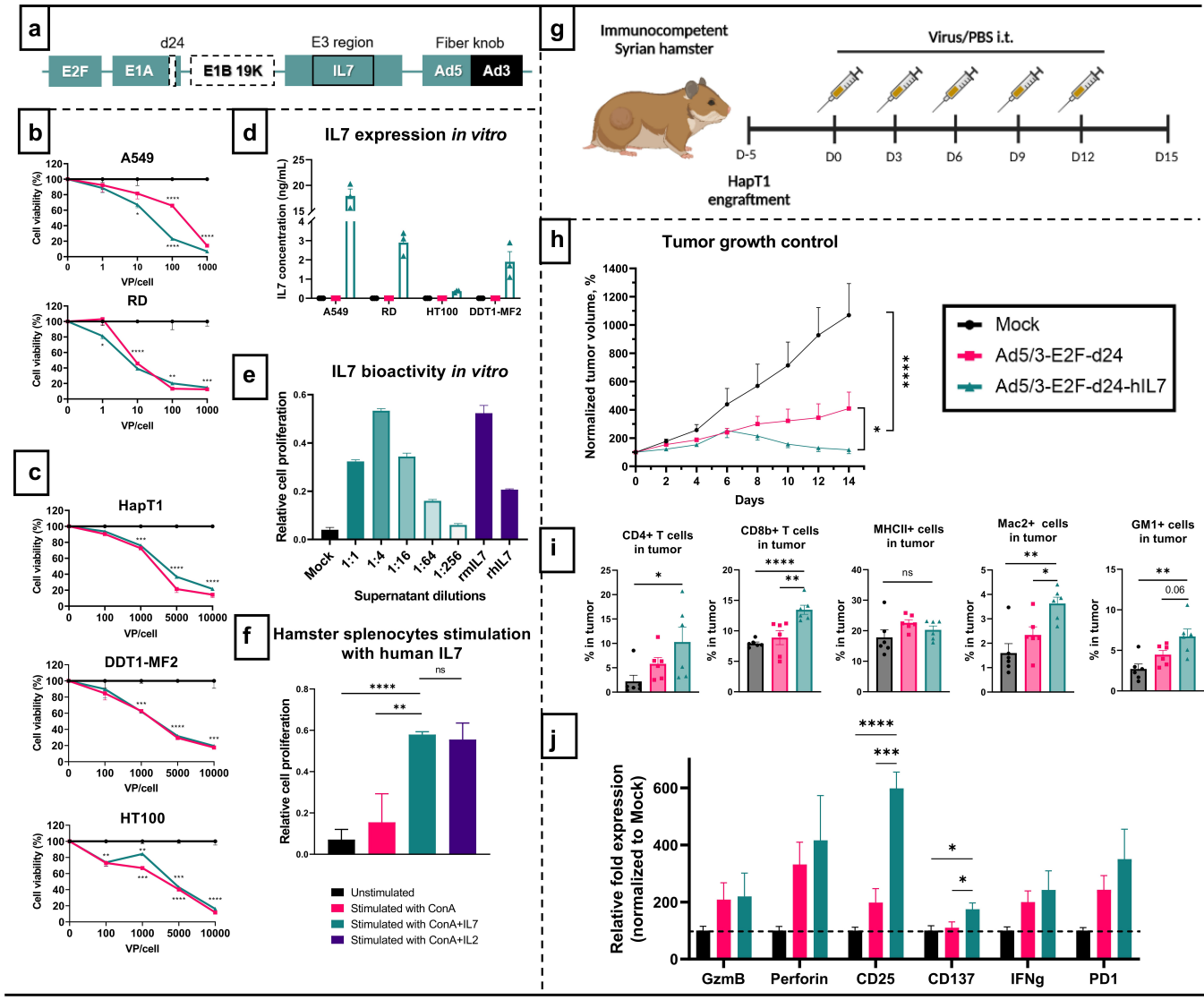

Figure 1. Ad5/3-E2F-d24-IL7 functionality *in vitro* and *in vivo*. (a) A schematic presentation of chimeric 5/3 oncolytic adenovirus armed with human interleukin 7. (b) Relative human cancer cell viability after addition of 1, 10, 100 or 1000 VP/cell at day 4 after infection in A549 and RD cell lines. (c) Relative hamster cancer cell viability after addition or 100, 1000, 5000 or 10000 VP/cell at day 5 after infection in HT100 and DDT1-MF2 or, at day 8 after infection in HapT1 cell lines. (d) Level of IL7 in the infected cancer cell supernatants. (e) IL7 bioactivity measured via application of infected cells supernatant on IL7-dependent murine cell line 2E8 in different dilutions. Recombinant murine IL7 (rmIL7) and murine IL7 (rhIL7) were used as controls at 20 ng/ml. (f) Human IL7 cross-reactivity in hamster splenocytes proliferation. All *in vitro* experiments were carried out in triplicates and repeated at least twice. Data is presented as mean ± SEM. (g) Schematic representation of syngeneic hamster experimental model. (h) Tumor growth until day 14. Tumor volumes were normalized against day 0. Data is presented as mean ± SEM. (i) Immune cells infiltrating treated tumors: CD4 + T cells, CD8 + T cells, MHC II expressing cells, GM-1+ cells (marker of NK cells), and Mac-2+ cells (marker of monocytes/macrophages). Data is presented as mean ± SEM. (j) Immune-related gene expression changes in tumor digests. Data is presented as mean ± SEM. Statistical significance is represented as *p < .05, **p < .01, ***p < .001, and ****p < .0001.

of tumor volumes, however IL7 coding virus-treated animals had notably smaller tumors than mock and Ad5/3-E2F-d24-treated animals ($p < .0001$ and $p = .0463$, respectively) (Figure 1h). Importantly, no side effects were observed and none of the treatments caused histopathological changes in normal hamster tissues (lungs, hearts, kidneys, livers, and spleens) 55 days after treatments started.

To gain a better understanding of the immunological mechanism of action of the IL7 armed adenovirus, we evaluated the frequency and diversity of tumor-infiltrating immune cells. We observed significantly higher number of CD8b+ T cells ($p = .0077$) and monocyte/macrophages (Mac-2 + cells) ($p = .0125$) (Figure 1i) in the IL7 virus treated tumors compared to unarmed virus. Number of CD4 + T cells and Asialo-GM1+ NK cells was higher in IL7 virus-treated group, but not statistically significant, while no difference was observed in the number of MHC class II+ cells. Interestingly, we observed significantly higher number of CD8b+ T cells ($p = .0362$), MHCII+ cells ($p = .0284$) and higher number of CD4 + T cells in blood (Supplementary figure S1A). No major differences between virus-treated groups were observed in splenocytes, except higher number of Mac2+ monocytes/macrophages ($p = .0125$) (Supplementary figure S1B).

Additionally, we measured the expression level of several immune-related genes in tumors harvested from animals. We observed substantial upregulation of canonical T cell activation markers CD25 ($p = .002$) and CD137 ($p = .0293$) in IL7 virus-treated group compared to backbone (Figure 1j). IFNg, Perforin

and PD1 showed upward trend in IL7 group, however the difference was not significant. No major differences were observed in the level of Granzyme B between virus-treated groups.

In conclusion, we showed that Ad5/3-E2F-d24-hIL7 virus treatment leads to effective *in vivo* tumor regression and enables the increased frequency of important immune cell subtypes and activation of relevant immune-stimulating factors.

Oncolytic adenovirus armed with IL7 infects and replicates in patient-derived *ex vivo* tumor cultures.

To further investigate the mechanism of action of the oncolytic adenovirus armed with IL7, we shifted toward more clinically relevant *ex vivo* tumor models. For this, we studied 3 samples of high grade serous carcinoma of fallopian tube (stage IVB), named as HUSOV4, OvCaS and HUSOV5 (Table 1). As expected, cell viability tests showed comparable lytic ability for both the backbone and IL7 encoding virus in all samples: after 3 days of incubation the viability reduced to 70–80% and continued to decrease until day 7 (Figure 2a).

Next, we evaluated the virus copy number in *ex vivo* tumor samples via quantitative real-time PCR targeting the E4 gene of the adenovirus. Overall, the amount of the viral DNA was comparable between the backbone and IL7 encoding virus across all tested samples (Figure 2b). However, there was clear difference in the total viral copy number between the samples: OvCaS and HUSOV5 produced the highest amount of virus DNA, whereas in HUSOV4 the virus concentration was roughly 100 times lower (Figure 2b).

Finally, we measured the human IL7 concentration in cancer culture supernatants. In all tested samples, we saw an increase in IL7 concentration from day 1 to day 3, however, as expected, the amount of protein was different across the samples. HUSOV4 and HUSOV5 samples had higher amount of IL7 reaching 0.57 and 0.35 pg/ug of total protein respectively, while IL7 concentration in OvCaS sample was at least 3 times lower and reached only 0.13 pg/ug of total protein (Figure 2c).

Overall, this data shows the ability of IL7 coding oncolytic adenovirus to infect, replicate and lyse patient-derived tumor digests, despite the biological differences between the samples.

Oncolytic adenovirus armed with IL7 creates an immunostimulating local tumor microenvironment

In order to evaluate the immune status of infected patient-derived *ex vivo* ovarian cancer samples, we measured the concentration of key immune signaling molecules in the cell culture supernatants 3 days after infection. First, we compared the level of proinflammatory cytokines: IL2, TNFa, IFNg and IL1b (Figure 3a). All tested samples showed statistically significant increase of IFNg when infected with IL7 encoding virus compared to uninfected cells and/or backbone virus group (p = .087 and 0.0351 for HUSOV4, p = .0009 and 0.0011 for OvCaS and p = .0065 and 0.0078 for HUSOV5, respectively). When infected with IL7 virus, OvCaS samples also displayed higher expression of IL2 (p = .0021 and 0.0320, respectively) and TNFa (p = .0017 and 0.0133, respectively) compared to uninfected cells and mock (Figure 3a). HUSOV4 and HUSOV5 did not exhibit other marked cytokine changes across the different experimental groups. No changes in the level of IL1b were observed in all tested samples. Overall, the level of pooled proinflammatory cytokines in OvCaS and HUSOV5 was notably higher in IL7 virus-treated group compared to other groups (Figure 3b).

Next, we measured the level of anti-inflammatory cytokines: IL4, IL6, IL10 and TGFb (Figure 3c). Overall, no significant increase of cytokine levels was observed in virus-treated groups compared to uninfected cells. HUSOV4 demonstrated a notable reduction in IL4, IL6 and IL10 concentration, while OvCaS and HUSOV5 had reduced amount of TGFb upon infection with IL7 encoding virus. The level of pooled anti-inflammatory cytokines was decreased in 2 out of 3 samples (OvCaS and HUSOV5) in cultures infected with the IL7 encoding virus (Figure 3d). The reduction was statistically significant between IL7 encoding virus and mock and backbone in the OvCaS sample (p = .0048 and 0.0398 respectively) (Figure 3d). Importantly, the IL-7 encoding virus induced the highest prevalence of proinflammatory cytokines over anti-inflammatory ones in all tested ovarian cancer patient samples (Figure 3e).

Overall, these data showed the ability of Ad5/3-E2F-d24 -hIL7 to induce the production of signaling molecules for converting the tumor microenvironment toward proinflammation, a status associated with the activation of T cells.

Table 1. Characteristics of the patient samples used in the study.

Patient ID	Age	Gender	Tumor Type	Diagnosis	Resection	Location
HUSOV4	79	F	Ovarian	High grade serous carcinoma St IVB	metastasis	Greater Omentum
OvCaS	61	F	Ovarian	High grade serous carcinoma St IVB	metastasis	Greater Omentum
HUSOV5	76	F	Ovarian	High grade serous carcinoma St IVB	metastasis	Greater Omentum
HUSOV10	65	F	Ovarian	High grade serous carcinoma St IVB	metastasis	Greater Omentum
HUSLU1	73	M	Lung	Adenocarcinoma, pT3N0M0	primary	Left lung lower lobe
HUSLU5	67	F	Lung	Adenocarcinoma, T4N0M0	primary	Right lung lower lobe
HUSHN15	81	F	Head and Neck	Squamous cell carcinoma, cT3N1M0 Still grade 2	primary	Base of tongue
HUSHN17	54	F	Head and Neck	Squamous cell carcinoma, T3N3bM0 StIVB	primary	Tongue
RCC2	52	F	Renal Cell	Clear cell renal cell carcinoma, pT3aN1	primary	Left kidney

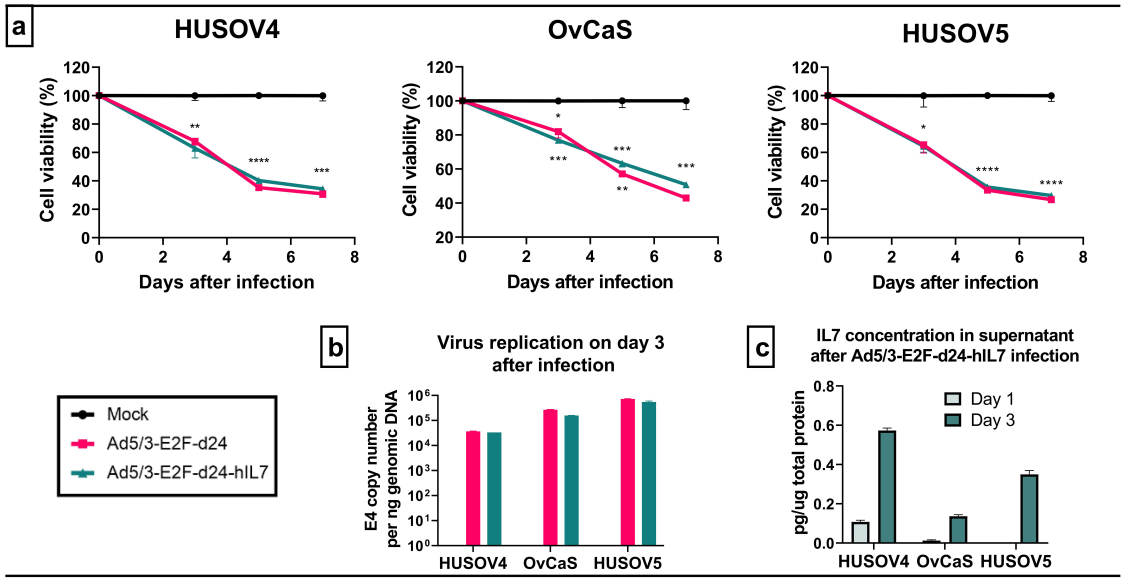

Figure 2. Lytic capability and replication of IL7 armed adenovirus in cancer patient *ex vivo* tumor cultures (a) Viability of tumor digests HUSOV4, OvCaS and HUSOV5 from ovarian cancer. Cell viability data is normalized against the uninfected mock. Experiments were performed in triplicates. Statistical significance is represented as *p < .05, **p < .01, ***p < .001, and ****p < .0001. (b) Ad5/3 replication evaluation through quantitative real-time PCR from ovarian samples. Viral copy number was normalized against human β-actin. PCRs were carried out in duplicates. (c) IL7 protein concentration in supernatants from ovarian samples, measured by Cytokine Bead Array (CBA) assay. Experiment was carried out in triplicates. All data is presented as mean ± SEM.

Oncolytic adenovirus armed with IL7 enables T cell migration to the tumor site

Besides measuring the levels of cytokines, we measured the level of chemokines in *ex vivo* infected ovarian cancer samples: Ccl2, Ccl5, Cxcl9, Cxcl10. Most notably, virus-treated samples showed remarkable increase in Ccl5 and Cxcl10 production, wherein IL7 encoding virus yielded significantly higher production than the backbone (Figure 3f). HUSOV4 sample did not show any other changes in chemokines concentration across the groups, while OvCaS sample additionally showed upregulation of Ccl2 and Cxcl9 when treated with IL7 encoding virus. HUSOV5 sample showed notable upregulation of Ccl5, Cxcl9 and Cxcl10 upon infection with IL7 encoding virus.

Since these chemokines are the main attractors for T cells, we next tested whether the change in chemokine concentrations can affect the migration of immune cells in OvCaS and HUSOV5 samples. Indeed, the absolute count of migrated immune cells was significantly higher in both samples treated with IL7 virus compared to mock and backbone (for OvCaS p = .0009 and 0.0127, respectively; for HUSOV5 p = .0389 and 0.0441, respectively) (Figure 3g).

Moreover, we characterized the populations of migrated cells. In OvCaS treated with Ad5/3-E2F-d24-hIL7 the frequency of migrated CD4+ and CD8+ cells was statistically significantly higher than in mock and Ad5/3-E2F-d24 treated group (for CD4+ cells p = .0038 and p < .0001, respectively; for CD8+ cells p = .0025 and 0.0014, respectively) (Figure 3h). In HUSOV5 treated with IL7 virus the number of CD4+, CD8 + cells as well as NK cells were significantly higher than in mock and Ad5/3-E2F-d24 treated group (for CD4+ cells p < .0001 and 0.0001, respectively; for CD8+ cells p < .0001 both; for NK cells p = .0090 and 0.0309, respectively) (Figure 3h).

Altogether, these data showed the ability of Ad5/3-E2F-d24-hIL7 to induce the production of functional chemokines and the *ex vivo* recruitment of immune cells (CD4+, CD8+, NK cells).

Oncolytic adenovirus armed with IL7 activates infiltrating CD4+ and CD8+ T cells in multiple cancers in a dose-dependent manner

To evaluate the effect of Ad5/3-E2F-d24-hIL7 on tumor-infiltrating lymphocytes, we first verified the expression level of activation and cytotoxic markers separately on CD4+ and CD8 + cells from HUSOV4, OvCaS and HUSOV5 *ex vivo* tumor cultures treated with the oncolytic adenoviruses via flow cytometry. Upon infection with the IL7 encoding virus, HUSOV4 and HUSOV5 cultures showed a significant increase in the amount of CD69+ CD4 + T cells (for HUSOV4 p = .0082 and 0.0094, respectively; for HUSOV5 p = .0020 and 0.0075, respectively) (Figure 4a) and CD69+ CD8 + T cells compared to mock and backbone groups (for HUSOV4 p = .0031 and 0.0013, respectively; for HUSOV5 p = .0116 and 0.0059, respectively) (Figure 4f). OvCaS sample showed similar trend, but the difference was not significant. Moreover, we observed higher frequency of IFNg +CD4+ cells (Figure 4b) as well as IFNg+CD8+ cells (Figure 4g) in HUSOV4 and HUSOV5 cultures treated with Ad5/3-E2F-d24-hIL7 compared to mock and Ad5/3-E2F-d24 groups.

On the transcriptome level we observed substantial upregulation of activation-associated genes, such as *HBEGF, MAP3K8, OSM, TNFSF8 (CD40LG), FLT3LG, ALOX5, TXK, IRF4*, in IL7 virus treated samples, however, CD4+ cells showed higher number of markers compared to CD8+ cells (Figure 4e and Figure 4j, respectively). Moreover, the inflammation-associated genes (*IL2RB, IL18R1, CEACAM1, CREM, FRMD4B*) were also upregulated in IL7 virus treated group compared to mock.

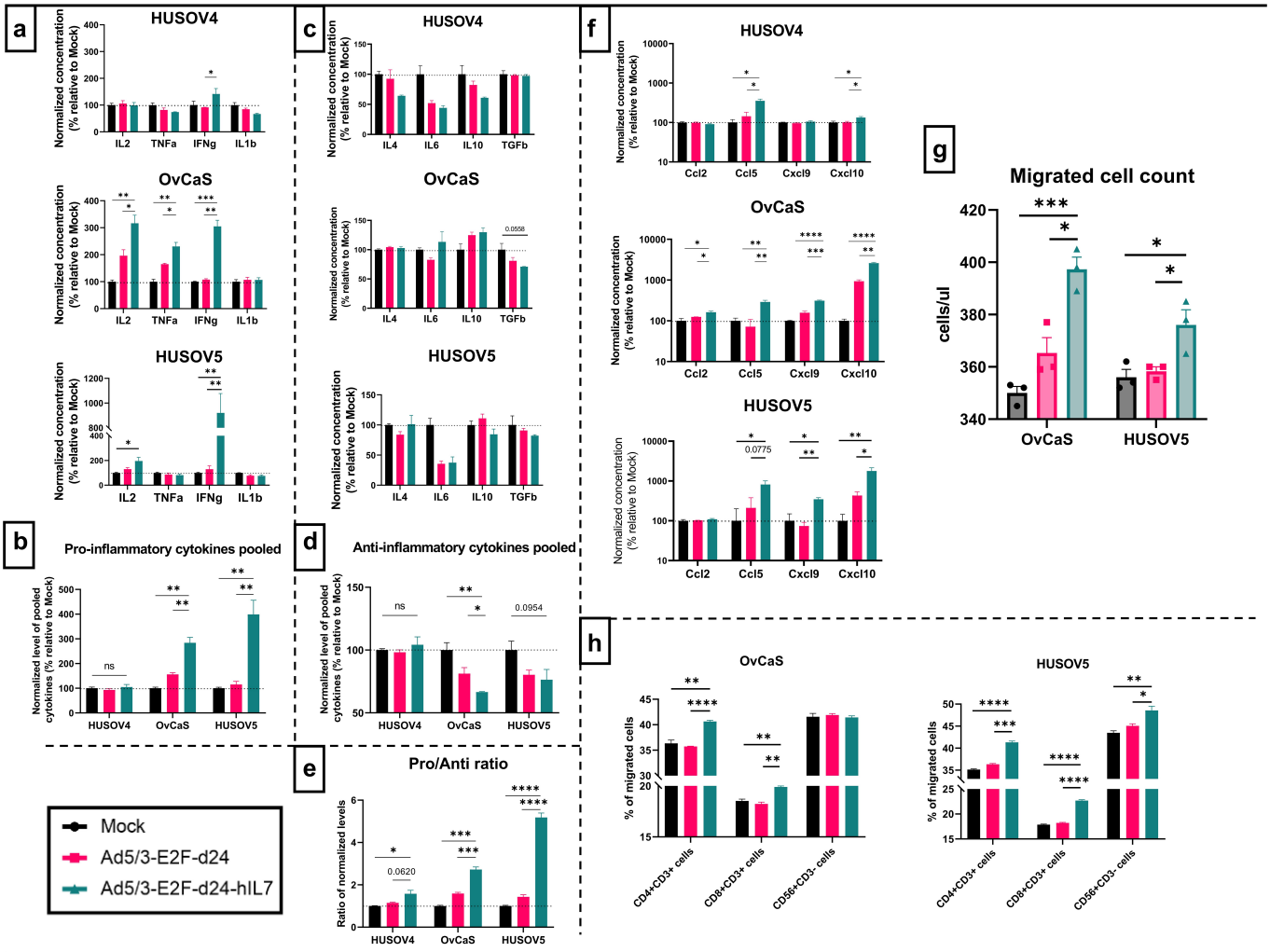

Figure 3. Evaluation of cytokines and chemokines in tumor microenvironment of ovarian cancer *ex vivo* tumor histocultures (HUSOV4, OvCaS and HUSOV5) upon viral infection. (a) Level of pro-inflammatory cytokines. (b) Pooled pro-inflammatory changes. (c) Level of anti-inflammatory cytokines. (d) Pooled anti-inflammatory changes. (e) Overall ratio of pro- to anti-inflammatory cytokines. Data was normalized against mock. (f) Level of chemokines. Data was normalized against mock. (g) Absolute number of migrated cells assessed using a Transwell system (5 μM pore membrane). The supernatant with cytokines and chemokines obtained after infection was added to the lower chamber. PBMCs were plated in the top chamber, and after 24 hours the number of cells at the bottom (migrated cells) were counted using 123count eBeads (Invitrogen). (h) Migrated immune cells profiling. All experiments were performed in triplicates, and resulting data is presented as mean ± SEM. Statistical significance is represented as *p < .05, **p < .01, ***p < .001, and ****p < .0001.

Next, we evaluated the changes in the proportion of cytotoxic T cells expressing Perforin (Perf), Granzyme B (GzmB) and TNFa – potent cytotoxic agents. In contrast to mock and backbone virus, in HUSOV4 and HUSOV5 cultures treated with IL7 encoding virus, we observed a notable increase of GzmB+ T cells, both CD4+ cells (Figure 4c) and CD8+ cells (Figure 4h) and an upward trend in TNFa+ CD4 + T cells (Figure 4d). All 3 cultures treated with Ad5/3-E2F-d24-hIL7 also showed an upward trend in frequency of Perf+CD8+ cells, however, only in HUSOV5 the difference was statistically significant compared to mock (p = .0002) and backbone group (p = .0052) (Figure 4i).

Interestingly, on transcriptome level we observed an upregulation of many cytotoxic markers in CD4+ cells (*GZMB, GZMH, PRF1, TNF, NKG7, CCR2, PRDM1*), but only three in CD8+ cells (*LTA, LTB, NCR3*). Notably, in contrast with CD4+ cells, we observed increased regulatory transcription factors *FOXP3, BACH2* and *MYBL2* expression in CD8+ cells. Additionally, both CD4+ cells and CD8+ cells showed upregulation of survival-associated genes *BCL2, PIM1* and *PDE4B*.

Moreover, we verified our previous observation of higher number of migrated cells in the samples treated with IL7 virus by the upregulation of migration-associated genes *ADAM19, DPP4, ITGA4, CCR5, SOS1* and *MYO1G* in CD4 + T cells and *ADAM19, FURIN* and *DPP4* in CD8+ cells (Figure 4e and Figure 4j, respectively).

To understand whether Ad5/3-E2F-d24-hIL7 treatment is cancer-specific, we additionally tested one more ovarian cancer sample and 5 patient-derived samples of different origin: two lung cancer samples HUSLU1 and HUSLU5, two head and neck cancer samples HUSHN15 and HUSH17 and one renal cell carcinoma sample RCC2 (Table 1). Overall, we observed increased amount of GzmB+CD4+ cells in all samples treated with IL7 encoding virus (Figure 5a) and did not find any correlation between the cell frequencies and IL7 concentration (Figure 5e). However, number of IFNg+CD4+, IFNg+CD8+ and CD69+ CD8+ was different across the samples (Figure 5b, 5c and 5d, respectively) and statistically significant correlated with IL7 concentration in the sample (Figure 5f, 5g and 5h, respectively).

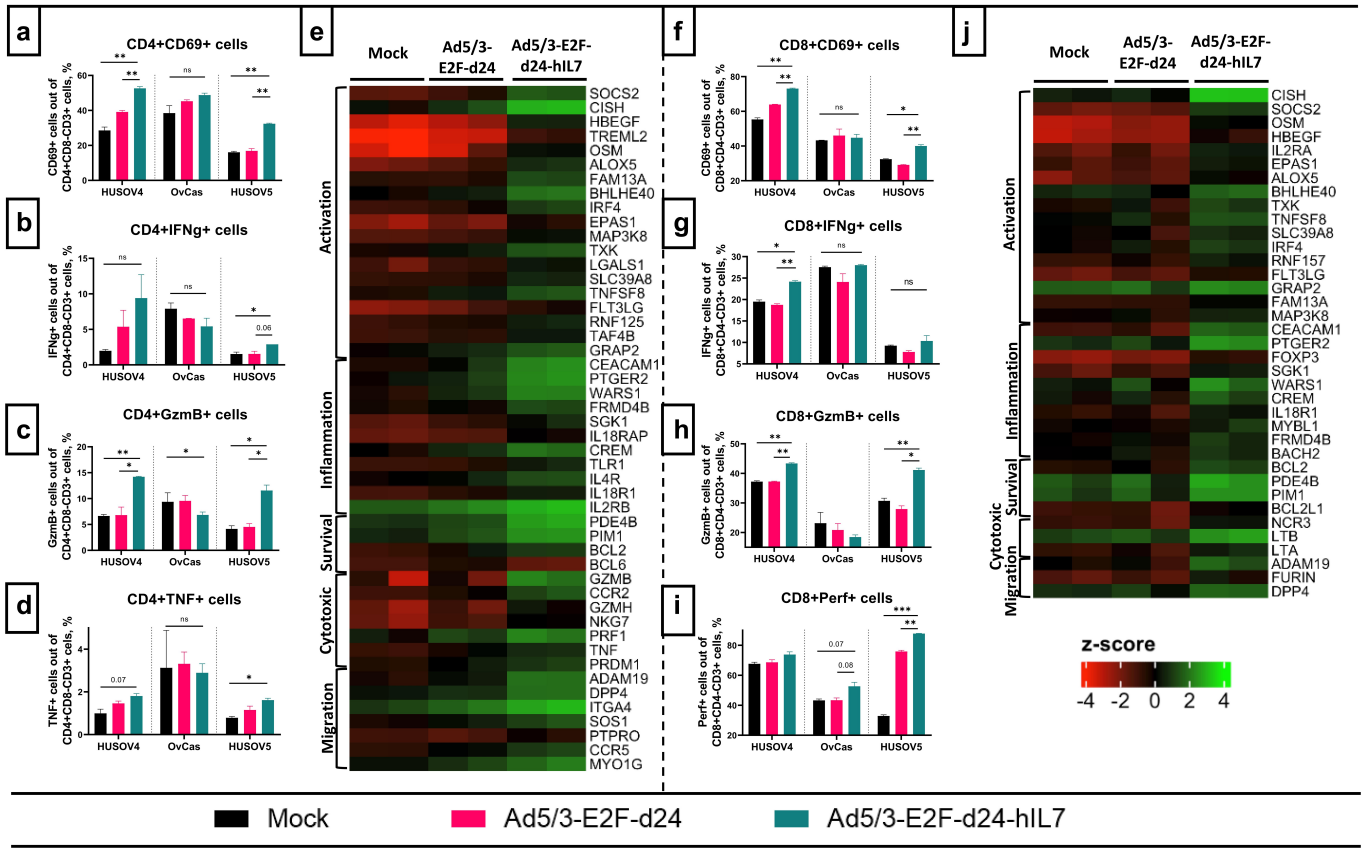

Figure 4. Evaluation of infiltrating CD4+ and CD8 + T cell activation and cytotoxicity in ovarian cancer *ex vivo* histocultures (HUSOV4, OvCaS and HUSOV5) upon viral infection. (a) Frequency of CD69+ cells, (b) IFNg+ cells, (c) GzmB+ cells and (d) TNF+ cells in CD4 + T cell populations measured through flow cytometry. (e) Differentially expressed genes in CD4 + T cell population. (f) Frequency of CD69+ cells, (g) IFNg+ cells, (h) GzmB+ cells and (i) Perf+ cells in CD8 + T cell populations measured through flow cytometry. (j) Differentially expressed genes in CD8 + T cell population. All flow cytometry experiments were run in duplicates, and resulting data is presented as mean ± SEM. Statistical significance is represented as *p < .05, **p < .01 and ***p < .001.

Overall, this data suggests the ability of Ad5/3-E2F-d24-hIL7 to activate infiltrating CD4+ cells and, to a lesser extent, CD8+ cells and to increase the proportion of cytotoxic immune cells in a dose-dependent manner.

Activated infiltrating CD4+ and CD8+ T cells are able to re-express IL7 receptor

We evaluated the presence of IL7 receptor chain α (IL7Ra) on the surface of the T cells. In both CD4+ and CD8+ cells from Ad5/3-E2F-d24-hIL7 treated cancer cultures we observed the upregulation of *CISH* and *SOCS2* genes (Figure 4e and Figure 4g, respectively), which are involved in the receptor internalization and degradation (Figure 5i). This data was supported by flow cytometry results showing a decrease in IL7Ra+ cells on day 1 upon infection on both CD4+ (Figure 5j) and CD8+ cells (Figure 5k). However, we observed gradual increase in IL7Ra+CD4+ and ILRa +CD8+ cells frequency until day 7 (Figure 5j and 5k, respectively). Interestingly, on day 7 number of GzmB+IL7Ra+CD4+ cells and CD69+ IL7Ra+CD4+ cells, which can be considered as previously activated cells, was higher than on days 1 and 3 (Figure 5l).

This data suggests that infiltrating CD4+ and CD8+ cells are able to re-express IL7 receptor after treatment with Ad5/3-E2F-d24-hIL7, and at least CD4+ remain activated and exhibit cytotoxic phenotype.

IL7 oncolytic adenovirus promotes tumor regression in a patient-derived xenograft (PDX) model via proliferation and activation of immune cells

The *in vivo* efficacy of Ad5/3-E2F-d24-hIL7 was additionally tested in more translationally relevant PDX model. Additionally, we compared two available immunodeficient models – NOG and NOG-IL2, the latter expressing human IL2 for improving reconstitution of patient matched immune cells following transfer.

PDX-OvCa cell line was engrafted subcutaneously into mice (5 animals per group) with subsequent intraperitoneal infusion of autologous PBMCs followed by intratumoral virus injections (Figure 6a). After 6 rounds of treatment, NOG mice in the IL7 virus-treated group had significantly smaller tumors when compared to mock group ($p < .0001$) and unarmed virus ($p = .0001$) (Figure 6b). Next, we evaluated the frequency and diversity of tumor-infiltrating and circulating immune cells. We observed significant higher number of CD4 + T cells ($p = .0364$), and CD8+ tumor-infiltrating cells ($p = .0497$) (Figure 6c) in the IL7 virus treated tumors compared to mock. Moreover, we observed a positive trend in immune cell frequency between unarmed virus-treated group and IL7 virus-treated group, although the difference was not significant. The proportion of activated CD69+ CD4+ cells was similar across all groups, however, IL7 virus treated animals

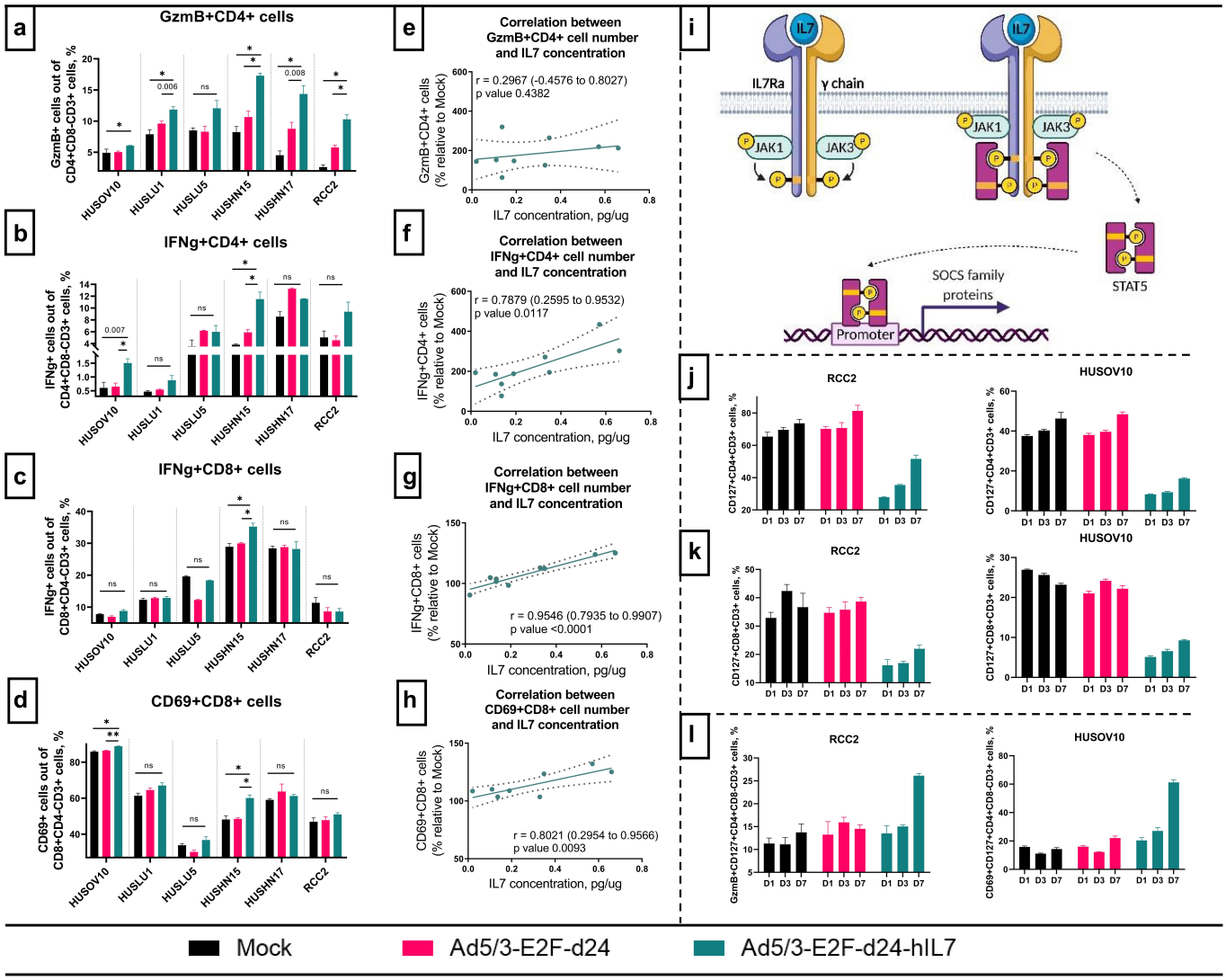

Figure 5. Evaluation of infiltrating CD4+ and CD8 + T cell activation, cytotoxicity and IL7Ra expression in multiple *ex vivo* samples and correlation with IL7 levels. (a) Frequency of GzmB+CD4+ cells, (b) IFNg+CD4+ cells, (c) IFNg+CD8+ cells and (d) CD69+ CD8+ cells in tumor microenvironment measured through flow cytometry. (e) Correlation between IL7 concentration and frequency of GzmB+CD4+ cells, (f) IFNg+CD4+ cells, (g) IFNg+CD8+ cells and (h) CD69+ CD8+ cells in tumor microenvironment (i) Mechanism of IL7Ra internalization. Briefly, interaction of IL7 with IL7Ra induces the heterodimerization of and conformational changes in IL7Rα and common gamma-chain receptor (γ chain). These conformational changes bring together tyrosine kinases Jak1 and Jak3, which phosphorylate each other, thereby increasing their kinase activity. Subsequently, the activated Jak proteins phosphorylate tyrosine residue Y449 in the cytoplasmic domain of IL7Ra creating a docking site for downstream effectors, for instance, signal transducer and activator of transcription 5 (STAT5). Phosphorylated STAT5 then homodimerizes and translocates to the nucleus, where it activates the expression of SOCS proteins, which are involved in cytokine signaling silencing, e.g. targeting receptor for internalization and degradation. (j) IL7Ra expression level on the surface of CD4+ cells and (k) CD8+ cells on day 1, 3 and 7 upon viral infection, measured through flow cytometry. (l) Expression of activation markers GzmB and CD69 on the CD127+ CD4+ cells on day 1, 3 and 7 upon viral infection, measured through flow cytometry. All flow cytometry experiments were run in duplicates, and resulting data is presented as mean ± SEM. Statistical significance is represented as *p < .05, **p < .01.

had more activated CD69+ CD8+ cells compared to mock (p = .0455) and to unarmed virus-treated mice (p = .0695) (Figure 6d). Additionally, measuring the number of immune cells circulating in the blood, we found significant increase of CD4+ cell in animals, treated with IL7 armed virus compared to mock (p = .0007) and backbone group (p = .0025), while no clear difference was observed for CD8+ cells (Figure 6e).

NOG-IL2 mice showed similar trend to the tumor reduction, although more moderate: in the IL7 virus-treated group tumors were significantly smaller when compared to mock group (p < .0001) and unarmed virus (p = .0029) (Figure 6f). We observed higher number of CD4 + T cells (p = .016) and activated CD69+ CD4+ cells (p < .0001) in tumors, while the proportion of CD8+ cells and activated CD69+ CD8+ cells remained similar across all groups (Figure 6g and 6h, respectively). We also did not find any difference in the number of circulating immune cells (Figure 6i).

In conclusion, we showed the ability of Ad5/3-E2F-d24-hIL7 virus to cause tumor regression via improved immune cells proliferation and infiltration in two translationally relevant ovarian PDX models.

Discussion

IL7 is well known as a homeostatic cytokine enabling T cell proliferation in lymphopenic hosts.[8,13] Subcutaneous administration of recombinant glycosylated hIL7 (CYT107, RevImmune,

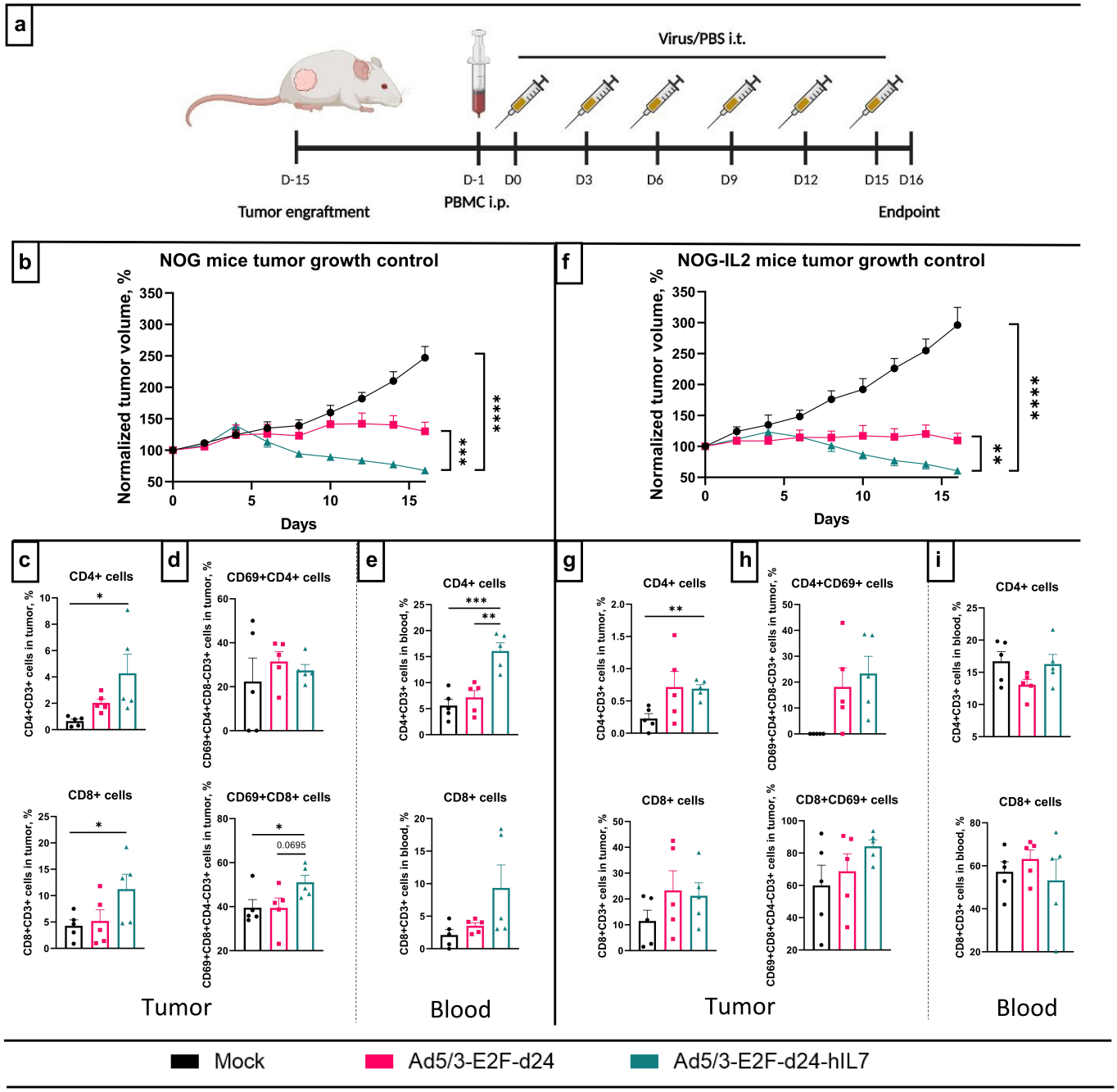

Figure 6. Ad5/3-E2F-d24-hIL7 efficacy in two distinct *in vivo* models bearing an ovarian PDX. (a) Schematic representation of PDX murine experimental model. (b) NOG mice tumor growth until day 15. Tumor volumes were normalized against day 0. Data is presented as mean+SEM. (c) Frequency of CD4+ and CD8+ cells and (d) CD69+ CD4+ and CD69+ CD8+ tumor infiltrating cells in NOG mice. (e) Frequency of circulating CD4+ and CD8+ in NOG mice. (f) NOG-IL2 mice tumor growth until day 15. Tumor volumes were normalized against day 0. Data is presented as mean+SEM. (g) Frequency of CD4+ and CD8+ cells and (h) CD69+ CD4+ and CD69+ CD8 + tumor infiltrating cells in NOG-IL2 mice. (i) Frequency of circulating CD4+ and CD8+ in NOG-IL2 mice. All flow cytometry experiments were run in duplicates, and resulting data is presented as mean ± SEM. Statistical significance is represented as *p < .05, **p < .01, ***p < .001, and ****p < .0001.

France) showed significant expansion of circulating T cells and mild to moderate adverse events in patients with metastatic melanoma and sarcoma,[8] breast cancer[13] and prostate cancer.[25] Although these studies were not designed to evaluate anti-tumor activity, one subject with central nervous system hemangiopericytoma and abdominal metastases had a substantial improvement of abdominal pain and a 20% reduction in tumor size at 3 months. The abdominal disease remained stable for 9 months after rhIL7 therapy.[8] Later on, Merchant et al. showed the efficacy of adjuvant IL7 therapy to improve survival in patients with metastatic pediatric sarcoma, although treatment efficacy was associated with histologic type of tumor.[26] This clinical data demonstrates that IL7 therapy continues to be an attractive anti-cancer approach, however its efficacy is limited, most likely due to insufficient IL7 concentration within the tumor.

In this study we created an oncolytic adenovirus armed with human IL7 allowing transgene delivery and expression at the tumor site. *In vitro* data showed the ability of the virus to lyse

several types of human and hamster cancer cell lines as well as cause the production of bioactive human IL7. Interestingly, the concentration of IL7 significantly varied among the cell lines, most likely due to differences in cell permissiveness, virus replication time and number of virus entry receptors.

Our preclinical data highlights the benefits of intratumorally expressed human IL7. We confirmed that oncolytic adenovirus Ad5/3-E2F-d24-hIL7 stimulates T cells and improves their infiltration leading to better tumor control in three clinically relevant animal models. We observed higher number of tumor-infiltrating CD4+ and CD8+ cells in both the immunocompetent pancreatic cancer hamster model and humanized ovarian cancer murine PDX model, as well as upregulation of T cells activation markers, such CD69 and CD25. As a result, animals treated with the virus armed with IL7 showed significant decrease in tumor size compared to the animals treated with unarmed virus.

Moreover, comparing two available immunocompromised models NOG and NOG-IL2 (Taconic) we observed more moderate immune response difference between the virus-treated groups in the latter. Most likely, overexpression of human IL2 can generally improve virotherapy by additional activation of immune cells, however, as expected, high concentration of IL2 leads to the adverse events and all animals regardless of the group appeared unhealthy 16 days after PBMCs engraftment. Interestingly, despite smaller tumors, the frequency of infiltrating CD4+ and CD8 + T cells was not significantly different in virus treated groups, even if there was a positive trend in cell number in tumors, treated with Ad5/3-E2F-d24-hIL7. This can be explained by more active cancer cells lysis in IL7 virus treated group, and therefore lowered replication of the virus and reduced transgene concentration, making the difference between the viruses elusive.

Since the reagents and assays for hamsters and immunodeficient animals are limited, and there is a point in studying the hypothesis from a translational perspective, we continued with *ex vivo* samples obtained from ovarian cancer patients. We first focused on the samples of high-grade serous carcinoma, which make up the majority of epithelial ovarian cancer cases.[27] Most serous carcinomas are diagnosed at stage III (51%) or IV (29%), for which the 5-year cause-specific survival is 42% and 26%, respectively.[28] Standard therapy includes surgery followed by platinum-based chemotherapy, however, to date, several immunotherapy approaches have been considered as a potential ovarian cancer treatment.[29] The reason might be that epithelial ovarian cancers usually have high frequency of T cell infiltrates, but also high percentage of immunosuppressive cells, such as regulatory T cells (Tregs), myeloid-derived suppressor cells (MDSCs) and tumor-associated macrophages (TAMs).[29,30] Thus, converting tumor microenvironment toward immunostimulatory one with an IL7 coding virus might be required to improve patients' response rate and overall survival.

In this study, we established 3 *ex vivo* ovarian cancer cultures and infected them with either unarmed or IL7 armed viruses. We observed significant decrease in cell viability in all samples upon infection showing that Ad5/3-E2F-d24-hIL7 is able to infect and lyse cancer cells presented in tumors. Interestingly, the concentration of IL7 in the supernatants was different between the samples. The reason might lie in the different proportion and initial viability of cancer cells in the samples, which are necessary for virus dissemination and replication. In general, it is important to mention, that the observed variations between the samples were expected for patient tumors due to individual set of mutations and tumor heterogeneity, regarding proportions of cancer, stromal and immune cells, as well as different frequency of immune cell populations.

The analysis of the tumor microenvironment showed a clear shift toward proinflammatory signaling in *ex vivo* patient samples infected with Ad5/3-E2F-d24-hIL7, particularly, increased IFNg production, which, in turn, stimulates expression of Ccl5, Cxcl9 and Cxcl10 – key chemokines involved in the recruitment of T cells and NK cells. Indeed, we observed higher number of CD4+ and CD8+ migrated cells when used supernatants obtained after infection with IL7 armed virus. Transcriptomic analysis showed upregulation of several migration-related genes in CD4+ cells – *CCR5, DPP4, ITGA4, MYO1G*. Interestingly, we observed significant upregulation of *ADAM19* gene in both CD4+ and CD8 + T cell, however, the role of this particular protein in immune cells is still unclear. ADAM proteins are membrane disintegrins and metalloproteinases, which convert nearby membrane-anchored cytokine precursors, cytokine receptors, Notch receptors, phagocytic receptors or cell adhesion molecules into soluble bioactive mediators.[31] In T cells, ADAMs can be involved in cell development and activation via cleavage of negative regulatory proteins, such as LAG3,[32] and regulate cell migration not only due to the proteolytic activity of ADAMs on the T cells themselves, but also due to the protease activity on the tissue cells serving as substrate of cell migration.[33] Nevertheless, additional experiments are needed to understand the role of *ADAM19* in T cells activation and migration upon Ad5/3-E2F-d24-hIL7 infection.

Further study of *ex vivo* patient samples showed the ability of the virus armed with IL7 to increase the number of polyfunctional cytotoxic CD4 + T cells expressing serine protease Granzyme B in two samples out of three. This finding was verified by RNAseq data showing higher expression of cytotoxic markers *GZBM, GZMH, NKG7, PRF1* and *TNF* in the samples treated with Ad5/3-E2F-d24-hIL7. Importantly, we didn't observe FOXP3 upregulation in CD4 + T cells, but decreased expression of *BCL6* and higher expression of *PRDM1*, encoding the transcriptional repressor Blimp-1, which are involved in CD4+ cells differentiation toward cytotoxic phenotype.[34–36] CD8 + T cells showed moderate activation capacity, in contrast to CD4+ cells. Despite similar signature, the number of differentially expressed genes upon IL7 virus infection in CD8+ cells was lower. Moreover, due to higher frequency of transcriptional factors *FOXP3, BACH2* and *MYBL1* transcripts in Ad5/3-E2F-d24-hIL7 treated group, CD8+ cells exhibited a regulatory phenotype rather than an effector phenotype.[37,38] CD8 + T regs is a very small population of regulatory immune cells which is not well described yet. One study claimed these cells only mildly suppress T cell proliferation and IFN-γ production,[39] compared to classic CD4+ CD25+ FoxP3 + T regs. Thus, we cannot say if the upregulation of FoxP3 in CD8+ cells correlates with severe immunosuppression.

Further, we analyzed more patient derived samples of different origin: lung, head and neck and renal cell cancer. As expected, we observed increased number of cytotoxic GzmB+CD4+ cells in all samples, however, the number of IFNg+ CD4+ and CD8+ cells was different among the samples. As we described earlier, the concentration of IL7 may differ depending on the number of cancer cells in the sample, and we found a positive correlation between IL7 concentration and number of activated IFNg+ T cells. Interestingly, we did not find any other correlations, *e.g.* cancer type, sample viability or amount of immune cells. Moreover, most likely CD4+ cells outcompete CD8+ cells when the IL7 concentration is limited, which lead to lesser activation of CD8+ cells.

Another important aspect of IL7 stimulation is the re-expression of IL7 receptor α chain (IL7Ra) on the surface of T cells. Upon activation, naïve T cells rapidly downregulate the receptor due to expression of SOCS proteins, which are involved in receptor internalization and degradation,[40,41] thus becoming effector functions. However, CD4+ and CD8+ cells can steadily re-express IL7Ra exhibiting memory cells phenotype, but both continue to be dependent on IL7 for their long-term survival.[42] We observed IL7Ra re-expression on these cells on day 7 after viral infection, while the frequency of IL7Ra+CD4 + cells were higher. Moreover, we did not observe any proliferation of CD4+ and the population of IL7Ra+CD4+ showed significant increase in Granzyme B and CD69 expression on day 7, which can be further explained by re-expression of the receptor by already activated cells. Altogether, our data shows the importance of high IL7 expression level for T cell priming, in other words, high Ad5/3-E2F-d24-hIL7 virus concentrations and/or repeated treatments are potentially beneficial for immune cell activation and therefore for tumor cell elimination.

In conclusion, our data demonstrates the ability of the new oncolytic adenovirus armed with IL7 to stimulate CD4 + T cells, and to a lesser extent CD8 + T cells, and improve their recruitment to the tumor site. This led to higher proportion of tumor-infiltrating lymphocytes and better tumor control in immunocompetent hamster pancreatic cancer and immunocompromised murine ovarian cancer models. The mechanism of action of Ad5/3-E2F-d24-hIL7 can be explained through improved activation and survival of immune cells as well as generation of cytotoxic CD4+ cells.

However, we believe it is possible to achieve even better anticancer and immunostimulatory response from the Ad5/3-E2F-d24-hIL7 treatment. Due to current model limitations, like semi-permissiveness of hamster cells, limited reagents for studies, immunodeficient models lacking competent immune system or short observation time of *ex vivo* samples, we could evaluate only early activated T cells, thus, additional studies are needed to elucidate the impact of TILT-517 on other lymphoid and myeloid cells. For example, several murine models were reported to be semi-permissive for the adenoviruses and support the transgenes expression in the tumor microenvironment.[43,44] Thus, using fully immunocompetent mice might be a reasonable solution to collect the data from B cells, NK cell, T regs and other suppressive cells, such as myeloid-derived suppressive cells and M2 macrophages. Of critical importance is to evaluate effector and central memory cells and, therefore, the generation of immunological memory and, as a result, better survival, and reduced probability of tumor relapse. Moreover, murine models make possible the depletion study which is essential for the understanding of main cell populations responsible for the anti-tumor response.

Additionally, we believe the combination of Ad5/3-E2F-d24 -hIL7 with immune checkpoint inhibitors (ICIs) is a promising approach to increase the potency of the latter. Based on our data, TILT-517 is able to convert tumor microenvironment into immunostimulatory one and attract immune cells, thus improving the efficacy of ICIs which tend to work only in "hot" tumors. An important aspect is the ability of IL7 to prevent T cells exhaustion by decreasing the expression of PD-1 receptor on the surface of the cells.[45,46] Thus, the combination with aPD-1 antibody might be a good strategy to get better therapeutic outcome in tumor types showing impaired T cell function, such as pancreatic[47] or metastatic renal cell cancer.[48]

Another interesting question regarding combination of aPD-1 and Ad5/3-E2F-d24-hIL7 is the possible better antitumor response in non-injected tumors. Recent study showed better antitumor response in non-injected tumors in animals treated with oncolytic adenovirus in combination with aPD-1,[49] however, in the context of IL7-induced immune memory cell formation, the abscopal effect might be additionally improved via combination of aPD-1 and Ad5/3-E2F-d24-hIL7.

Overall, based on our data, arming of adenoviruses with IL7 is appealing and this approach can be translated to the clinic, however, additional studies should be performed to evaluate full potential of the novel virus.

Acknowledgments

We thank Minna Oksanen and Riikka Kalliokoski for expert experimental and administrative assistance and Marjukka Anttila for her help with histopathological evaluation of the tissue samples. We also thank Dmitrii Bychkov, Annabrita Schoonenberg and FIMM digital microscopy and molecular pathology unit (University of Helsinki, Helsinki, Finland), Laboratory Animal Center (LAC, University of Helsinki, Helsinki, Finland) and Biomedicum Flow Cytometry Unit (University of Helsinki, Helsinki, Finland). Additionally, we thank Taconic Biosciences GmbH (Leverkusen, Germany) for the help with animal models. Open access funded by the Helsinki University Library (University of Helsinki, Finland).

Disclosure statement

No potential conflict of interest was reported by the author(s).

Funding

This study was supported by Doctoral programme in clinical research (University of Helsinki), Jane and Aatos Erkko Foundation, HUCH Research Funds (VTR), Finnish Cancer Organizations, Novo Nordisk Foundation, Päivikki and Sakari Sohlberg Foundation and TILT Biotherapeutics Ltd;Marie Sklodowska-Curie;Doctoral programme in clinical research, University of Helsinki, Finland;Suomen Kulttuurirahasto;TILT Biotherapeutics Ltd.;

ORCID

Akseli Hemminki http://orcid.org/0000-0001-7103-8530

Ethics statement

All animal experiments described in the paper were approved by the Provincial Government of Southern Finland and the Experimental Animal Committee of the University of Helsinki (license number ESAVI/12559/2021).

Cancer samples were collected from the patients undergoing surgical resection at the Helsinki University Central Hospital (HUS, Helsinki, Finland). Sample collection was approved by HUS Operatives Ethics Committee (permit numbers HUS/850/2017, HUS/3360/2019 and HUS/259/2021) and the patients gave their written consent.

Authors' contributions

- TVK, JC, DCAQ, JMS, RH, CH, IGN and AH designed the experiments;
- TVK, JC, DCAQ, JMS, SB, SP, SGVK and VA conducted the experiments;
- KA, LB, JR, II, KB, MR, OH, AR, AK and JT collected the patient samples;
- TVK, JC and AK analyzed the results;
- All the authors contributed to writing and reviewing the manuscript.

References

1. Fyfe G, Fisher RI, Rosenberg SA, Sznol M, Parkinson DR, Louie AC. Results of treatment of 255 patients with metastatic renal cell carcinoma who received high-dose recombinant interleukin-2 therapy. J Clin Oncol. 1995;13:688–696. doi:10.1200/JCO.1995.13.3.688.
2. Golomb HM, Ratain MJ, Mick R, Daly K. Interferon treatment for hairy cell leukemia: an update on a cohort of 69 patients treated from 1983-1986. Leukemia. 1992 Nov;6(11):1177–1180.
3. Kammula US, White DE, Rosenberg SA. Trends in the safety of high dose bolus interleukin-2 administration in patients with metastatic cancer. Cancer. 1998 Aug; 83(4):797–805. PMID: 9708948.
4. Kirkwood JM, Goldhirsch A, Barylak E, Borden E. Quality-of-life adjusted survival analysis of interferon alpha-2b adjuvant treatment of high-risk cutaneous melanoma: an eastern cooperative oncologyGroup study. J Clin Oncol. 1996;14:2666–2673. doi:10.1200/JCO.1996.14.10.2666.
5. Kirkwood JM, Strawderman MH, Ernstoff MS, Smith TJ, Borden EC, Blum RH. Interferon alpha-2b adjuvant therapy of high risk resected cutaneous melanoma: the eastern cooperative oncology group trial EST 1684. J Clin Oncol. 1996;14:7–17. doi:10.1200/JCO.1996.14.1.7.
6. Webb LM, Foxwell BM, Feldmann M. Putative role for interleukin-7 in the maintenance of the recirculating naive CD4+ T-cell pool. Immunology. 1999 Nov;98(3):400–405. doi:10.1046/j.1365-2567.1999.00906.x.
7. Sportès C, Hakim FT, Memon SA, Zhang H, Chua KS, Brown MR, Fleisher TAKrumlauf MC, Babb RR, Chow CK, Fry TJ, Engels J, Buffet R, Morre M, Amato RJ, Venzon DJ, Korngold R, Pecora A, Gress RE, Mackall CL. Administration of rhIL-7 in humans increases in vivo TCR repertoire diversity by preferential expansion of naive T cell subsets. J Exp Med. 2008 Jul 7;205(7):1701–1714. doi:10.1084/jem.20071681.
8. Rosenberg SA, Sportès C, Ahmadzadeh M, Fry TJ, Ngo LT, Schwarz SL, Stetler-Stevenson M, Morton KE, Mavroukakis SA, Morre M, Buffet R, Mackall CL, Gress RE. IL-7 administration to humans leads to expansion of CD8+ and CD4+ cells but a relative decrease of CD4+ T-regulatory cells. J Immunother. 2006May-Jun ;29(3):313–319. doi:10.1097/01.cji.0000210386.55951.c2.
9. Heninger AK, Theil A, Wilhelm C, Petzold C, Huebel N, Kretschmer K, Bonifacio E, Monti P. IL-7 abrogates suppressive activity of human CD4+CD25+FOXP3+ regulatory T cells and allows expansion of alloreactive and autoreactive T cells. J Immunol. 2012 Dec 15;189(12):5649–5658. doi:10.4049/jimmunol.1201286.
10. Pellegrini M, Calzascia T, Elford AR, Shahinian A, Lin AE, Dissanayake D, Dhanji S, Nguyen LT, Gronski MA, Morre M, et al. Adjuvant IL-7 antagonizes multiple cellular and molecular inhibitory networks to enhance immunotherapies. Nat Med. 2009 Jul;15(7):819. doi:10.1038/nm0709-819b.
11. Koyas A, Tucer S, Kayhan M, Savas AC, Akdemir I, Cekic C. Interleukin-7 protects CD8+ T cells from adenosine-mediated immunosuppression. Sci Signal. 2021 Mar 16;14:674. doi:10.1126/scisignal.abb1269.
12. Sportès C, RR B, Krumlauf MC, FT H, SM S, CK C, MR B, TA F, Noel P, Maric I, et al. Phase I study of rhIL7 administration in subjects with refractory malignancy. Clin Cancer Res. 2010 Jan 15;16(2):727–735. doi:10.1158/1078-0432.CCR-09-1303.
13. Trédan O, Ménétrier-Caux C, Ray-Coquard I, Garin G, Cropet C, Verronèse E, Bachelot T, Rebattu P, Heudel PE, Cassier P, et al. ELYPSE-7: a randomized placebo-controlled phase IIa trial with CYT107 exploring the restoration of CD4+ lymphocyte count in lymphopenic metastatic breast cancer patients. Ann Oncol. 2018 Feb 1;29(2):523. doi:10.1093/annonc/mdx058.
14. Lee SW, Choi D, Heo M, Shin EC, Park SH, Kim SJ, Oh YK, Lee BH, Yang SH, Sung YC, et al. hIL-7-hyFc, A long-acting IL-7, increased absolute lymphocyte count in healthy subjects. Clin Transl Sci. 2020 Nov;13(6):1161–1169. doi:10.1111/cts.12800.
15. Markley JC, Sadelain M. IL-7 and IL-21 are superior to IL-2 and IL-15 in promoting human T cell-mediated rejection of systemic lymphoma in immunodeficient mice. Blood. 2010 Apr 29;115(17):3508–3519. doi:10.1182/blood-2009-09-241398.
16. Miller PW, Sharma S, Stolina M, Butterfield LH, Luo J, Lin Y, Dohadwala M, Batra RK, Wu L, Economou JS, et al. Intratumoral administration of adenoviral interleukin 7 gene-modified dendritic cells augments specific antitumor immunity and achieves tumor eradication. Hum Gene Ther. 2000 Jan 1;11(1):53–65. doi:10.1089/10430340050016157.
17. Nakao S, Arai Y, Tasaki M, Yamashita M, Murakami R, Kawase T, Amino N, Nakatake M, Kurosaki H, Mori M, et al. Intratumoral expression of IL-7 and IL-12 using an oncolytic virus increases systemic sensitivity to immune checkpoint blockade. Sci Transl Med. 2020 Jan 15;12(526):eaax7992. doi:10.1126/scitranslmed.aax7992.
18. Huang J, Zheng M, Zhang Z, Tang X, Chen Y, Peng A, Peng X, Tong A, Zhou L. Interleukin-7-loaded oncolytic adenovirus improves CAR-T cell therapy for glioblastoma. Cancer Immunol Immunother. 2021 Sep;70(9):2453–2465. doi:10.1007/s00262-021-02856-0.
19. Havunen R, Siurala M, Sorsa S, Grönberg-Vähä-Koskela S, Behr M, Tähtinen S, Santos JM, Karell P, Rusanen J, Nettelbeck DM, et al. Oncolytic adenoviruses armed with tumor necrosis factor alpha and interleukin-2 enable successful adoptive cell therapy. Mol Ther Oncolytics. 2016 Dec 31;4:77–86. doi:10.1016/j.omto.2016.12.004.
20. Sharan SK, Thomason LC, Kuznetsov SG, Court DL. Recombineering: a homologous recombination-based method of genetic engineering. Nat Protoc. 2009;4(2):206–223. doi:10.1038/nprot.2008.227.
21. Lock M, Korn M, Wilson J, Sena-Esteves M, Gao G. Measuring the infectious titer of recombinant adenovirus using tissue culture infection dose 50% (tcid50) end-point dilution and quantitative polymerase chain reaction (qPCR). Cold Spring Harb Protoc. 2019 Aug 1;2019:8. doi:10.1101/pdb.prot095562.
22. Santos JM, Heiniö C, Cervera-Carrascon V, Quixabeira DCA, Siurala M, Havunen R, Butzow R, Zafar S, de Gruijl T, Lassus H, et al. Oncolytic adenovirus shapes the ovarian tumor microenvironment for potent tumor-infiltrating lymphocyte tumor reactivity. J Immunother Cancer. 2020 Jan;8(1):e000188. doi:10.1136/jitc-2019-000188.

23. Jin J, Sabatino M, Somerville R, Wilson JR, Dudley ME, Stroncek DF, Rosenberg SA. Simplified method of the growth of human tumor infiltrating lymphocytes in gas-permeable flasks to numbers needed for patient treatment. J Immunother. 2012;35(3):283–292. doi:10.1097/CJI.0b013e31824e801f.
24. Han J, Sabbatini P, Perez D, Rao L, Modha D, White E. The E1B 19K protein blocks apoptosis by interacting with and inhibiting the p53-inducible and death-promoting Bax protein. Genes Dev. 1996 Feb 15;10(4):461–477. doi:10.1101/gad.10.4.461.
25. Pachynski RK, Morishima C, Szmulewitz R, Harshman L, Appleman L, Monk P, Bitting RL, Kucuk O, Millard F, Seigne JD, et al. IL-7 expands lymphocyte populations and enhances immune responses to sipuleucel-T in patients with metastatic castration-resistant prostate cancer (mCRPC). Journal for ImmunoTherapy of Cancer. 2021;9:e002903. doi:10.1136/jitc-2021-002903.
26. Merchant MS, Bernstein D, Amoako M, Baird K, Fleisher TA, Morre M, Steinberg SM, Sabatino M, Stroncek DF, Venkatasan AM, et al. Adjuvant immunotherapy to improve outcome in high-risk pediatric sarcomas. Clin Cancer Res. 2016;22(13):3182–3191. doi:10.1158/1078-0432.CCR-15-2550.
27. IeM S, Kurman RJ. Ovarian tumorigenesis: a proposed model based on morphological and molecular genetic analysis. Am J Pathol. 2004;164(5):1511–1518. doi:10.1016/S0002-9440(10)63708-X.
28. Torre LA, Trabert B, DeSantis CE, Miller KD, Samimi G, Runowicz CD, Gaudet MM, Jemal A, Siegel RL. Ovarian cancer statistics, 2018. CA Cancer J Clin. 2018 Jul;68(4):284–296. doi:10.3322/caac.21456.
29. Yang C, Xia BR, Zhang ZC, Zhang YJ, Lou G, Jin WL. Immunotherapy for ovarian cancer: adjuvant, combination, and neoadjuvant. Front Immunol. 2020 Oct;6(11):577869. doi:10.3389/fimmu.2020.577869.
30. Santoiemma PP, Reyes C, Wang LP, McLane MW, Feldman MD, Tanyi JL, Powell DJ Jr. Systematic evaluation of multiple immune markers reveals prognostic factors in ovarian cancer. Gynecol Oncol. 2016 Oct;143(1):120–127. doi:10.1016/j.ygyno.2016.07.105.
31. Lambrecht BN, Vanderkerken M, Hammad H. The emerging role of ADAM metalloproteinases in immunity. Nat Rev Immunol. 2018 Dec;18(12):745–758. doi:10.1038/s41577-018-0068-5.
32. Li N, Wang Y, Forbes K, Vignali KM, Heale BS, Saftig P, Hartmann D, Black RA, Rossi JJ, Blobel CP, Dempsey PJ. Metalloproteases regulate T-cell proliferation and effector function via LAG-3. EMBO J. 2007;26(2):494–504. doi:10.1038/sj.emboj.7601520.
33. Dreymueller D, Theodorou K, Donners M, Ludwig A. Fine tuning cell migration by a disintegrin and metalloproteinases. Mediators Inflamm. 2017;2017:9621724. doi:10.1155/2017/9621724.
34. Hua L, Yao S, Pham D, Jiang L, Wright J, Sawant D, Dent AL, Braciale TJ, Kaplan MH, Sun J. Cytokine-dependent induction of CD4+ T cells with cytotoxic potential during influenza virus infection. J Virol. 2013 Nov;87(21):11884–11893. doi:10.1128/JVI.01461-13.
35. Śledzińska A, Vila de Mucha M, Bergerhoff K, Hotblack A, Demane DF, Ghorani E, Akarca AU, Marzolini MAV, Solomon I, Vargas FA, et al. Regulatory T cells restrain interleukin-2- and blimp-1-dependent acquisition of cytotoxic function by CD4+ T cells. Immunity. 2020 Jan 14;52(1):151–166.e6. doi:10.1016/j.immuni.2019.12.007.
36. Fu SH, Yeh LT, Chu CC, Yen BLJ, Sytwu H-K. New insights into Blimp-1 in T lymphocytes: a divergent regulator of cell destiny and effector function. J Biomed Sci. 2017;24:49. doi:10.1186/s12929-017-0354-8.
37. Roychoudhuri R, Hirahara K, Mousavi K, Clever D, Klebanoff CA, Bonelli M, Sciumè G, Zare H, Vahedi G, Dema B, et al. BACH2 represses effector programs to stabilize T(reg)-mediated immune homeostasis. Nature. 2013 Jun 27;498(7455):506–510. doi:10.1038/nature12199.
38. Best J, Blair D, Knell J, Yang E, Mayya V, Doedens A, Dustin ML, Goldrath AW. Transcriptional insights into the CD8+ T cell response to infection and memory T cell formation. Nat Immunol. 2013;14:404–412. doi:10.1038/ni.2536.
39. Mayer CT, Floess S, Baru AM, Lahl K, Huehn J, Sparwasser T. CD8+ Foxp3+ T cells share developmental and phenotypic features with classical CD4+ Foxp3+ regulatory T cells but lack potent suppressive activity. Eur J Immunol. 2011 Mar;41(3):716–725. doi:10.1002/eji.201040913.
40. Krebs DL, Hilton DJ. SOCS proteins: negative regulators of cytokine signaling. Stem Cells. 2001;19:378–387.
41. Mazzucchelli R, Durum SK. Interleukin-7 receptor expression: intelligent design. Nat Rev Immunol. 2007;7:144–154. doi:10.1038/nri2023.
42. Barata JT, Durum SK, Seddon B. Flip the coin: IL-7 and IL-7R in health and disease. Nat Immunol. 2019;20:1584–1593. doi:10.1038/s41590-019-0479-x.
43. Zhang L, Hedjran F, Larson C, Perez GL, Reid T. A novel immunocompetent murine model for replicating oncolytic adenoviral therapy. Cancer Gene Ther. 2015 Jan;22(1):17–22. doi:10.1038/cgt.2014.64.
44. Liu W, Wang X, Feng X, Yu J, Liu X, Jia X, Zhang H, Wu H, Wang C, Wu J, et al. Oncolytic adenovirus-mediated intratumoral expression of TRAIL and CD40L enhances immunotherapy by modulating the tumor microenvironment in immunocompetent mouse models. Cancer Lett. 2022 Mar 21;535:215661. doi:10.1016/j.canlet.2022.215661.
45. Hou L, Jie Z, Liang Y, Desai M, Soong L, Sun J. Type 1 interferon-induced IL-7 maintains CD8+ T-cell responses and homeostasis by suppressing PD-1 expression in viral hepatitis. Cell Mol Immunol. 2015 Mar;12(2):213–221. doi:10.1038/cmi.2014.49.
46. Teng D, Ding L, Cai B, Luo Q, Wang H. Interleukin-7 enhances anti-tumor activity of CD8+ T cells in patients with hepatocellular carcinoma. Cytokine. 2019 Jun;118:115–123. doi:10.1016/j.cyto.2018.04.003.
47. Saka D, Gökalp M, Piyade B, Cevik NC, Arik Sever E, Unutmaz D, Ceyhan GO, Demir IE, Asimgil H. Mechanisms of T-Cell Exhaustion in Pancreatic Cancer. Cancers (Basel). 2020 Aug 14;12(8):2274. doi:10.3390/cancers12082274.
48. Braun DA, Street K, Burke KP, Cookmeyer DL, Denize T, Pedersen CB, Gohil SH, Schindler N, Pomerance L, Hirsch L, et al. Progressive immune dysfunction with advancing disease stage in renal cell carcinoma. Cancer Cell. 2021 May 10;39(5):632–648.e8. doi:10.1016/j.ccell.2021.02.013.
49. Quixabeira DCA, Cervera-Carrascon V, Santos JM, Clubb JHA, Kudling TV, Basnet S, Heiniö C, Grönberg-Vähä-Koskela S, Anttila M, Havunen R, et al. Local therapy with an engineered oncolytic adenovirus enables antitumor response in non-injected melanoma tumors in mice treated with aPD-1. Oncoimmunology. 2022 Jan 22;11(1):2028960. doi:10.1080/2162402X.2022.2028960.